World Academy of Science, Engineering and Technology
International Journal of Electrical and Computer Engineering
Vol:12, No:11, 2018

Design of a Hand-Held, Clamp-on, Leakage Current Sensor for High Voltage Direct Current Insulators

Morné Roman, Robert van Zyl, Nishanth Parus, Nishal Mahatho

***Abstract*—**Leakage current monitoring for high voltage transmission line insulators is of interest as a performance indicator. Presently, to the best of our knowledge, there is no commercially available, clamp-on type, non-intrusive device for measuring leakage current on energised high voltage direct current (HVDC) transmission line insulators. The South African power utility, Eskom, is investigating the development of such a hand-held sensor for two important applications; first, for continuous real-time condition monitoring of HVDC line insulators and, second, for use by live line workers to determine if it is safe to work on energised insulators. In this paper, a DC leakage current sensor based on magnetic field sensing techniques is developed. The magnetic field sensor used in the prototype can also detect alternating current up to 5 MHz. The DC leakage current prototype detects the magnetic field associated with the current flowing on the surface of the insulator. Preliminary HVDC leakage current measurements are performed on glass insulators. The results show that the prototype can accurately measure leakage current in the specified current range of 1-200 mA. The influence of external fields from the HVDC line itself on the leakage current measurements is mitigated through a differential magnetometer sensing technique. Thus, the developed sensor can perform measurements on in-service HVDC insulators. The research contributes to the body of knowledge by providing a sensor to measure leakage current on energised HVDC insulators non-intrusively. This sensor can also be used by live line workers to inform them whether or not it is safe to perform maintenance on energized insulators.

***Keywords*—**Direct current, insulator, leakage current, live line, magnetic field, sensor, transmission lines.

I. Introduction

INSULATORS are vital components of overhead transmission lines and substations. Insulator and transmission line faults caused by bird excreta, pollution, contamination and lightning have a significant impact on the performance of high voltage (HV) transmission lines [1]. Light rain and high humidity increase the conductivity of insulators, which cause dry-band arcs and eventual flashover (electrical breakdown of the air) [2]-[4]. Line-faults involving insulator flashover, especially near the coast, therefore pose a major challenge to power utilities. The level of leakage current (LC) that flows on the insulator can therefore indicate conditions that are conducive for the onset of flashover [5]. LCs have also been known to degrade the insulation material, for example cracking of porcelain insulators, pin corrosion on glass insulators and the ageing of composite insulator shed material [6]. As a result, the measurement of LC on HV transmission lines has become important. While conventional current transformers (CTs) are used for the measurement of current [7], they cannot measure DC as there are no alternating fields to couple with the CT device.

The South African power utility, Eskom, requires a non-intrusive, in-situ monitoring solution to measure LC flowing on their HVDC transmission line insulators. For this purpose, the design and testing of a hand-held, clamp-on type sensor that can measure HVDC insulator LC are reported here. Real-time sensing of the LC can be used as a condition-based monitoring system for early detection of possible line faults. Measurements can also be used to classify safe and unsafe conditions for live line workers. In future, the prototype sensor will enable in depth analyses of LC safety limits.

II. AC and DC LC Sensing Techniques

Various techniques for insulator LC measurement exist. One technique uses fibre optics, whereby the LC modulates an ultra-bright light-emitting diode (LED) that produces a modulated light signal. This signal is transmitted via fibre optics to a remote unit [8]. CTs can be used to measure LC [9]; however, as pointed out earlier, CTs are only suitable for AC measurements. Chen et al. developed a non-intrusive current sensor based on the Rogowski coil principle that measures LC from a few Hertz to tens of MegaHertz [10]. This device, too, cannot perform DC measurements. Resistive shunts and online leakage current analysers (OLCAs) can measure both AC and DC current [11]-[13]. A glass stand-off insulator has to be installed in series with the insulator under test when an OLCA and resistive shunt are used. Thus, an OLCA and the resistive shunt are not practical for energised transmission lines as the insulator string will have to be de-energised and disconnected to install the stand-off. They are more suitable for controlled laboratory experiments.

Research shows that magnetic field sensors can be used to detect LC around energised insulators [14], [15]. The design and operational deployment of these sensors are heavily influenced by the harsh magnetic field environment around transmission lines. Eskom will eventually deploy the LC sensors in the Cahora Bassa HVDC transmission line system. The influence of the ambient magnetic environment, therefore, has to be mitigated.

The financial support of the National Research Foundation and the Eskom Research, Testing and Development department towards this research is acknowledged. Also, the South African National Space Agency for availing their facilities is acknowledged.

M. Roman and R. R. van Zyl are with the Electrical Engineering Department, Cape Peninsula University of Technology, Cape Town, South Africa (e-mail: romanm@cput.ac.za, vanzylr@cput.ac.za).

N. Parus and N. Mahatho are with the Research, Testing & Development Department, Eskom Holdings SOC Ltd, Johannesburg, South Africa (e-mail: nishanp@eskom.co.za, mahathn@eskom.co.za).

The objective of the sensor is to enable the measurement of a minimum LC of 1 mA on the insulator in the presence of the main line current, which is assumed to be 4 m from where the sensor will be clamped in position around the insulator (see Fig. 1).

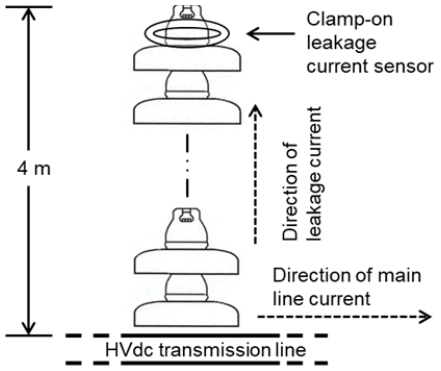

Fig. 1 Measurement setup showing position of LC sensor in relation to HVDC transmission line

III. LC Sensor Prototype with Single Magnetometer

A. Design

A DC LC sensor that is hand-held and can clamp around a cap of a glass insulator with a 100 mm diameter is required. The sensor should be capable of measuring LC in the range 1 - 200 mA on energised insulators, while being clamped approximately 4 m away from the HVDC line current that is rated at 1800 A for the Cahora Bassa transmission line. The DC LC sensor consists of the following components:

- Magnetoresistive (MR) 1-axis magnetometer;
- High permeability soft magnetic core; and
- Signal conditioning circuitry.

B. Measurements

Tests with the single magnetometer prototype were performed at Eskom's corona cage HV test facility to establish if it can measure LC flowing on an energised HVDC insulator's surface.

1) Determining the Prototype's V-I Curve

Calibration of the prototype is performed against a 10 Ω, 5 W shunt resistor reference measurement. Calibration entails adjusting the sensor's offset to zero and then adjusting its amplitude to be the same as the shunt resistor when injecting a current on the insulator under test. A known current (low voltage) is injected through the insulator setup. A wire is connected from the cap to the pin of the insulator (viz. a short circuit of the glass area of the insulator disc). Fig. 2 shows the measured V-I curves of the prototype LC sensor and shunt resistor.

The measurements show that the prototype is linear over the current range of interest and does not saturate. Furthermore, a measurement error of less than 1% is observed for both the shunt resistor and prototype sensor. The V-I curves will be used to determine the actual current that is flowing on the insulator during HVDC LC tests.

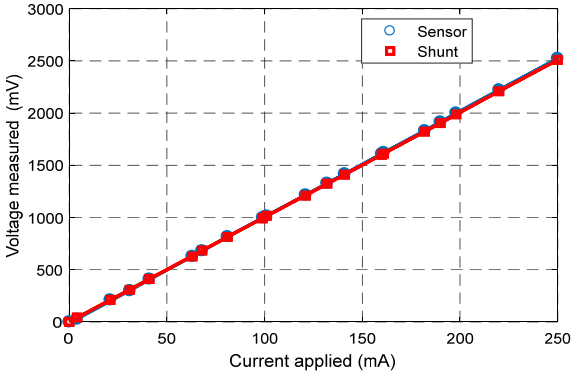

Fig. 2 V-I curves of prototype LC sensor and shunt resistor

2) LC Measurements on Energized, Polluted Glass Insulators

An HVDC power supply, with a 12 mA maximum rating, is used to generate LC on a polluted insulator after calibrating the prototype. Fig. 3 shows the test setup for the HV measurements. The insulator is sprayed with salt water to aid the flow of LC on the insulator's surface. The prototype is covered with aluminium and non-conductive material to protect its electronics from the sprayed salt water and to prevent LC from flowing on the aluminium of the prototype. The unprocessed measurement data are presented in Fig. 4.

C. Discussion of Results

Due to the nature of the response in Fig. 4, it can be split into separate regions (Region 1 and Region 2).

1) Region 1

This region essentially has a steady linear response, where the LC is proportional to the voltage. A discharge happens at 10 ms. This data are, however, not included in the linear region plot in Fig. 5. Fig. 5 compares the LC measurement of the prototype and the shunt resistor for Region 1. It also shows the scatter plot of the prototype and shunt resistor.

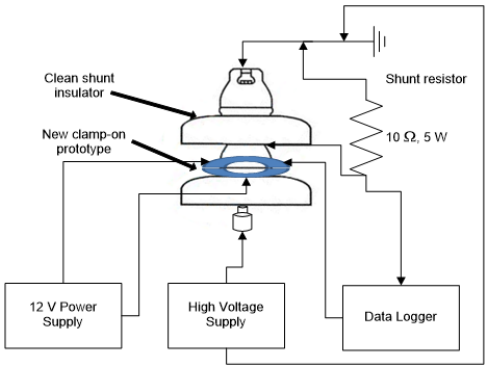

Fig. 3 Schematic diagram of LC measurement setup at Eskom's HV test facility

From Fig. 5 it is evident that the measurements of both sensors are correlated; the calculated correlation coefficient for the two sets is 0.98. Fig. 6 shows the histogram of the calculated error between the two measurement sets; the error distribution has an average and a standard deviation of 0.19

mA and 0.5 mA, respectively.

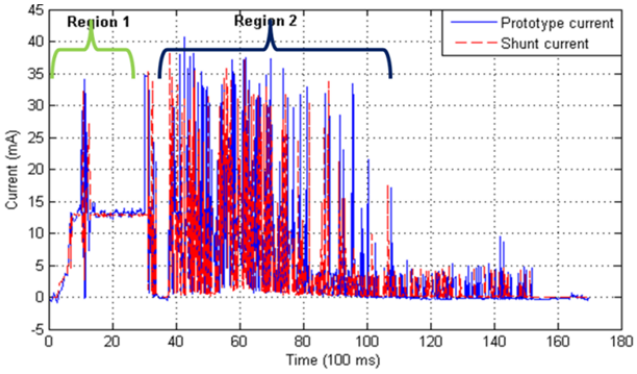

Fig. 4 LC measurements of the shunt resistor and prototype sensor (100 ms sampling rate)

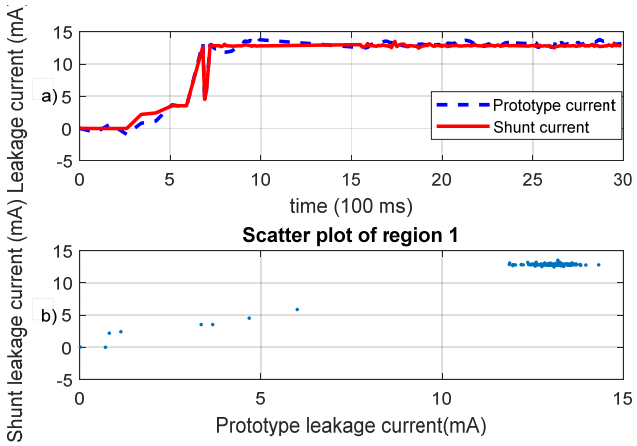

Fig. 5 (a) LC measurements of the shunt resistor and prototype sensor in Region 1, (b) Scatter plot of measurements presented in (a)

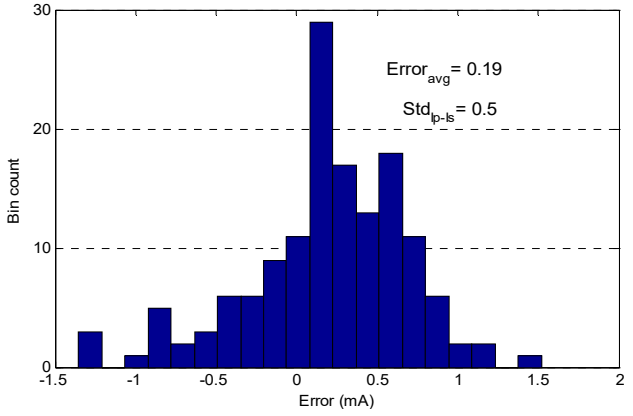

Fig. 6 Error distribution of LC measurements (Region 1)

1) Region 2

The measurements in Region 2 of both the shunt and prototype appear to be random as indicated by the scatter plot in Fig. 7. The apparent randomness depicted in Fig. 7 can be ascribed to under-sampling of the data. The observed discharges are current pulses that occur in the millisecond to nanosecond range [16]. Consequently, the sampling frequency should conform to Shannon's Theorem. Due to the data logger's limitations, the sampling rate was set at 100 ms, resulting in under-sampling. In future work, wideband time- and frequency-domain techniques will be investigated to study the partial discharges in more detail as described in [17].

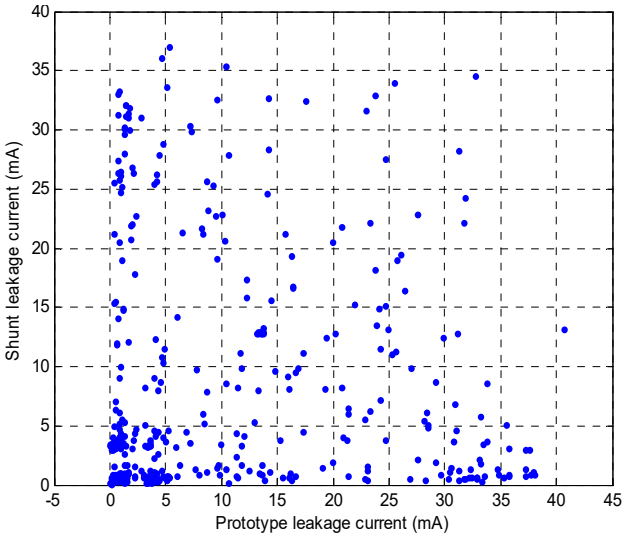

Fig. 7 Scatter plot of LC measurements with the prototype and shunt resistor in Region 2

Fig. 8 shows that the insulation tape, which forms part of the prototype's enclosure, was covered with salt pollution after the tests. This induced salt pollution is a phenomenon that was not anticipated, and that may have affected the results as LC may have flowed on the outside of the prototype.

Fig. 8 LC test setup showing the pollution on the outside of prototype and insulators (with two stand-off insulators)

In conclusion, the HVDC LC tests show that the prototype can detect and measure DC LC that is flowing on an insulator's surface even in the presence of discharges. However, for the HV pollution tests (Fig. 4), differences in the magnitude of the current pulses are noted.

IV. Adaptation of Prototype for In-Situ Measurements

A. Design

From Section III, it is evident that the prototype sensor can

measure LC. However, since it is based on a magnetometer, it will be influenced by the presence of ambient magnetic fields. The Cahora Bassa transmission line's magnetic field is of the order 10^3 higher than the insulator's LC magnetic field. Thus, in its previous form described in section 3, the prototype sensor is not suitable for in-situ measurements on energised insulators.

A differential magnetometer method (DMM) is implemented to mitigate the effect of external fields [18]. This method requires two DC LC sensors, both measuring the ambient magnetic field. However, one sensor will be clamped around the insulator or current carrying wire, and it will measure the fields of both the LC and the external ambient fields. The two sensors' outputs will be subtracted to remove the effect of the ambient magnetic field, leaving only the contribution of the actual LC from the insulator. Fig. 9 illustrates the DMM concept for LC measurement. Since the prototype needs to perform in-situ LC measurements on energised insulators, a clamp is designed for it. Fig. 10 shows the mechanical parts of the prototype on a glass insulator. The circuitry is designed to conform to the circumference of the core that measures only the ambient field (the core that remains closed).

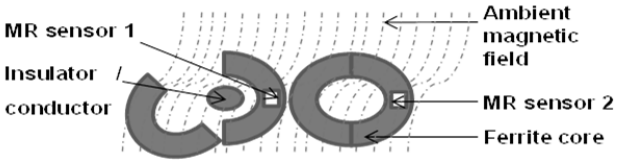

Fig. 9 Differential magnetometer method concept to detect LC

Fig. 10 Adapted prototype LC sensor with its mechanical clamps around a glass insulator

B. Calibration

The adapted prototype requires calibration in the presence of external magnetic fields equivalent to those that will be experienced in the Cahora Bassa scheme before in-situ measurements are performed on the energised insulators.

A 3-axis Helmholtz coil, with a 1 m^3 volume, has been used as calibration instrument since the prototype sensor is intrinsically based on magnetometers. The Helmholtz coil generates a predetermined magnetic field by injecting currents into the appropriate coils in each axis. A LEMI-011B fluxgate magnetometer determines the generated magnetic field within the centre working volume of Helmholtz coil. The coil system used can generate a magnetic field of up to 70 µT, which is sufficient for the current purposes.

Fig. 11 shows the coil system for calibration. The LEMI-011B fluxgate magnetometer is placed in the centre working volume. The measured B-I curve of the coil systems is presented in Fig. 12. The prototype is calibrated against this B-I curve.

Fig. 11 3-axes Helmholtz coil system for calibration of the prototype LC sensor

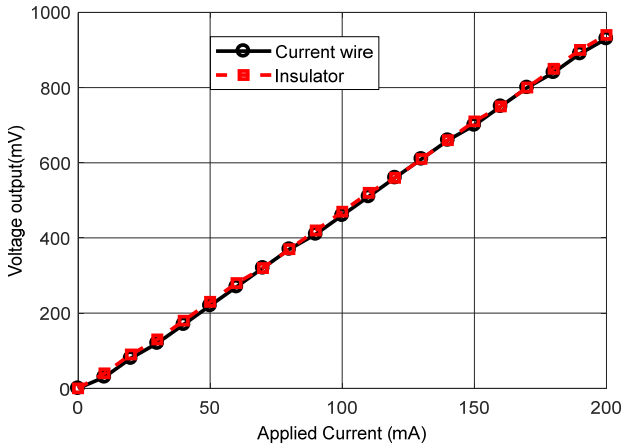

Fig. 12 DC LC measurements for the adapted prototype sensor in the presence of an external 70 µT field

C. Measurements

A linearity test is performed to generate the prototype's V-I characteristic curve that will be used by live line workers. The prototype performs LC measurements with, first, a current carrying wire and then a glass insulator placed within its circumference. A current supply injects LC into the wire and steps it in 10 mA increments to 200 mA. Simultaneously, the

Helmholtz coil generates a 70 μT field in all its axes while the prototype is measuring the current through the wire and on the insulator, representing the LC. The results are presented in Fig. 13 and show that the adapted prototype sensor is linear over the required current range, and is not influenced by the external field. The prototype has a sensitivity of ~ 4.5 mV / mA, which can be adjusted.

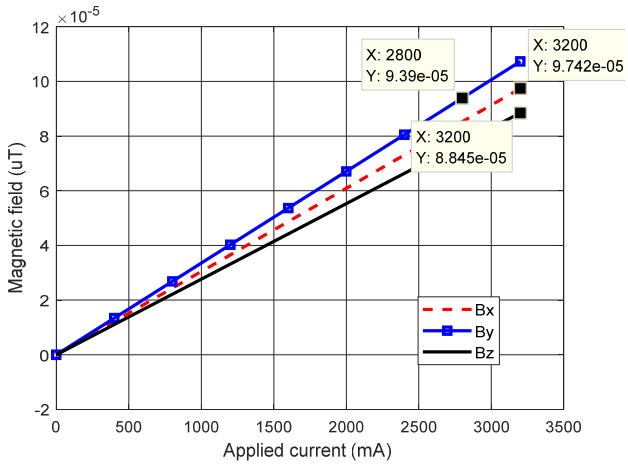

Fig. 13 Measured B-I curves for each of the axes of the 3-axis Helmholtz coil system

V. Conclusions and Recommendations

This paper discusses the development of a clamp-on non-intrusive DC LC sensor. In section 3, LC measurements are performed at Eskom's corona cage to observe if the single magnetometer prototype can measure the LC flowing on a glass insulator's surface. The tests verify that the prototype can indeed measure DC LC that is flowing on an insulator's surface, even in the presence of discharges. In section 4, a differential magnetometer method is implemented to mitigate the impact of external magnetic fields on the current sensor. This method requires two magnetometers. Calibration of the prototype LC sensor is performed in a Helmholtz coil. The results show that the adapted prototype sensor yields a linear measurement response over the required current range and is not influenced by an external field.

The next step in the ongoing research is the development of a new prototype (CAD model shown in Fig. 14), which will include a water-tight enclosure along with electromagnetic shielding. Also, remote data capturing is being investigated by connecting through a Wi-Fi module or VHF/UHF transceiver.

Fig. 14 CAD model of envisaged prototype

References

[1] W. K. Glossop, "Performance comparison of existing AC and DC transmission lines within Southern Africa with predictions for lines above 765kv", M.S. thesis, Dept. Eng. and built environment, Univ. of Witwatersrand, Johannesburg, 2008.

[2] C. Zchariades, S. M. Rowland, I. Cotton, "Real-time monitoring of leakage current on insulating cross-arms in relation to local weather conditions", *Electrical Insulation Conference*, Ottowa, ON, Canada, pp. 397-401, June 2013.

[3] L. H. Meyer, C. R. P. Oliboni, T. I. A. H. Mustafa, H. A. D. Almaguer, F. H. Molina, G. Cassel, "A study of the correlation of leakage current, humidity and temperature of 25 kV insulators in urban and rural areas", *Conference on Electrical Insulation and Dielectric Phenomena*, Cancun, Mexico, pp. 398-402, October 2011.

[4] Suwarno, J. Parhusip, "Effects of humidity and fog conductivity on the leakage current waveforms of ceramics for outdoor insulators", *WSEAS transaction on systems*, Vol. 9, Issue 4, pp. 442-452, 2010.

[5] Fluke. "Leakage current measurements basics", (Online). Available: http://www.fluke.com/fluke/uses/comunidad/fluke-news-plus/articlecategories/electrical/leakagebasics.

[6] L. Holtzhausen, J. P. Pieterse, H. J. Vermeulen, S., Limbo, "Insulator aging tests with HVAC and HVDC excitation using the tracking wheel tester", *International Conference. on High Voltage Engineering and Application (ICHVE 2010)*, New Orleans, LA, USA, pp. 445-448, October 2010.

[7] W. H. Schwardt, J. P. Holtzhausen, W. L. Vosloo, "A Comparison between measured leakage current and surface conductivity during salt fog tests", *7th Africon Conference in Africa, Gaborone*, Botswana, pp. 597-600, September 2004.

[8] M. M. Werneck, D. M. dos Santos, C. C. de Carvalho, F. V. B. de Nazare, R. C. S. Allil, "Detection and monitoring of leakage currents in power transmission insulators", *IEEE sensors journal*, pp. 1-9, 2014.

[9] A. J. Phillips, F. F. Bologna, J. M. Major, C. S. Engelbrecht, "Development and demonstration of low cost robust leakage current sensors for evaluating contaminated insulators", *Proceedings of the 16th International Symposium on High Voltage Engineering*, Cape Town, South Africa, paper 5-3, pp. 1-6, August 2009.

[10] W. Chen, C. Yao, P. Chen, C. Sun, L. Du, R. Liao, "A new broadband microcurrent transducer for insulator leakage current monitoring system", *IEEE Trans. on Power Delivery*, Vol. 23, Issue 1, pp. 355-360, 2008.

[11] Z. Jia, C. Chen, X., Wang, H. Lu, "Leakage current analysis on RTV coated porcelain insulators during long term fog experiments", *IEEE Trans. on Dielectrics and Electrical Insulation*, Vol. 21, Issue 4, pp. 1547-1553, 2014.

[12] P. J. Pieterse, A. I. Elombo, G. N. J. Mouton, H. J. Vermeulen, J. P. Holtzhausen, W. L. Vosloo, "A coastal insulator pollution test station for the evaluation of the relative ageing performance of power line insulators under AC and DC voltage", *Proceedings of the 17th International Symposium on High Voltage Engineering,* Hannover, Germany, C-007, pp. 1-5, August 2011.

[13] A. I. Elombo, J. P. Haultzhausen, H. J. Vermeulen, P. J. Pieterse, W. L. Vosloo, "Comparative evaluation of the leakage current and aging performance of HTV SR insulators of different creepage lengths when energised by AC, DC+, DC- in a severe marine environment", *IEEE Trans. on Dielectrics and Electrical Insulation,* Vol. 20, Issue 2, pp. 421-428, 2013.

[14] M. Roman, R. R. van Zyl, N. Parus, N. Mahatho, "A novel technique for measuring HVDC insulator leakage current using magnetic field sensors", *The 19th International Symposium on High Voltage Engineering*, http://www.zcu.cz/pracoviste/vyd/online/FEL_ISH_2015_Proceedings.zip, OF1, ID-36, Pilsen, Czech Republic, pp. 1-6, August 2015.

[15] M. Roman, R. R. van Zyl, N. Parus, N. Mahatho, "Insulator leakage current monitoring: challenges for high voltage direct current transmission lines", *in Industrial and Commercial Use of Energy (ICUE),* Cape Town, South Africa, pp. 1-7, August 2014.

[16] J. Sarkar, R. Patil. "Detection of partial discharges occurring in HVDC environment", *International journal of innovative science, engineering and technology*, Vol. 1, Issue 4, pp. 424-428, 2014.

[17] A. J. Otto, H. C. Reader. "Wideband and narrowband HVDC conductor corona test methods for radio noise prediction", *IEEE Trans. on Power Delivery*, Vol. 25, No. 4, pp. 2950-2957, 2010.

[18] E. Matandirotya, P. J. Cilliers, R.R. van Zyl R. "Methods of measuring

and modelling geomagnetically induced currents (GICs) in a power line", *Proceedings of SAIP2013, the 58th Annual Conference of the South African Institute of Physics*, edited by Roelf Botha and Thulani Jili (SAIP and University of Zululand), pp. 410-415, July 2013.